A Climatology of Nocturnal Low-Level Jets at Cabauw

P. BAAS, F. C. BOSVELD, AND H. KLEIN BALTINK

Royal Netherlands Meteorological Institute, De Bilt, Netherlands

A. A. M. HOLTSLAG

Meteorology and Air Quality, Wageningen University, Wageningen, Netherlands

(Manuscript received 19 February 2008, in final form 19 December 2008)

ABSTRACT

A climatology of nocturnal low-level jets (LLJs) is presented for the topographically flat measurement site at Cabauw, the Netherlands. LLJ characteristics are derived from a 7-yr half-hourly database of wind speed profiles, obtained from the 200-m mast and a wind profiler. Many LLJs at Cabauw originate from an inertial oscillation, which develops after sunset in a layer decoupled from the surface by stable stratification. The data are classified to different types of stable boundary layers by using the geostrophic wind speed and the isothermal net radiative cooling as classification parameters. For each of these classes, LLJ characteristics like frequency of occurrence, height above ground level, and the turning of the wind vector across the boundary layer are determined. It is found that LLJs occur in about 20% of the nights, are typically situated at 140–260 m above ground level, and have a speed of 6–10 m s^{-1}. Development of a substantial LLJ is most likely to occur for moderate geostrophic forcing and a high radiative cooling. A comparison with the 40-yr ECMWF Re-Analysis (ERA-40) is added to illustrate how the results can be used to evaluate the performance of atmospheric models.

1. Introduction

Low-level jets (LLJs) are frequently observed phenomena in the nocturnal atmosphere in many parts of the world. They are characterized by a maximum in the wind speed profile, which is typically situated 100–500 m above the earth's surface. In the literature, many studies can be found on the development and the characteristics of LLJs (e.g., Bonner 1968; Garratt 1985; Kraus et al. 1985; Whiteman et al. 1997; Andreas et al. 2000; Banta et al. 2002; Song et al. 2005).

Knowledge of the characteristics of the LLJ is relevant for aviation, wind energy applications (Storm et al. 2008), the transport of pollutants (Beyrich 1994), and other atmospheric constituents like ozone (Banta et al. 1998) and carbon dioxide (Mathieu et al. 2005; Karipot et al. 2006). Furthermore, the strong shear below the jet can influence the turbulent exchange between the surface and the atmosphere (Banta et al. 2006; Conangla and Cuxart 2006). Recent wind tunnel experiments showed that LLJ-generated shear may cause intermittent bursts of turbulence in the lower part of the stable boundary layer (SBL) (Ohya et al. 2008). Over the Great Plains in the United States, LLJs are related to large amounts of moisture transport (Cheinet et al. 2005), which plays an important role in the formation of deep convective systems (Maddox 1983).

Modeling of the SBL is still a challenge (e.g., Holtslag 2006). In addition to breaking gravity waves, radiation divergence, and sensitivity to surface heterogeneity, LLJs also complicate an accurate prediction of the SBL (e.g., Mahrt et al. 1998). Stensrud (1996) suggests that the structure of the SBL is closely linked to characteristics of the LLJ. Banta et al. (2003) state that bulk properties of the LLJ must be represented correctly in atmospheric models to obtain realistic vertical turbulent mixing characteristics. At the same time, the parameterization of turbulent diffusion for stable stratification is important for simulating the LLJ.

Currently, general circulation models (GCMs) are not able to reproduce properties of the LLJ in a satisfactory way (Cheinet et al. 2005). This is especially true for LLJs that form below 200 m above the surface

Corresponding author address: P. Baas, Royal Netherlands Meteorological Institute, Atmospheric Research, Wilhelminalaan 10, P.O. Box 201, 3730 AE, De Bilt, Netherlands.
E-mail: peter.baas@knmi.nl

DOI: 10.1175/2009JAMC1965.1

(Banta et al. 2002). LLJs at higher levels have been successfully simulated as shown by, for example, Anderson and Arritt (2001) and Castro et al. (2007). For the Great Plains area they find that, in comparison with long-term observations from the National Oceanic and Atmospheric Administration (NOAA) Wind Profiler Network (lowest level of detection at 500 m above ground level), the representation of LLJs in the National Centers for Environmental Prediction–National Center for Atmospheric Research (NCEP–NCAR) reanalysis is generally realistic. Ghan et al. (1996) find similar results for a comparison of two GCMs with Bonner's (1968) climatology. Apart from climatological studies as mentioned above, many studies investigate one or more individual LLJ cases, for example, to learn about its forcings or to test different parameterization schemes (e.g., Parish et al. 1988; Zhong et al. 1996; Zhang et al. 2001; Storm et al. 2008; Todd et al. 2008).

This study presents a climatology of the nocturnal LLJ at Cabauw, the Netherlands. Having such a climatology available, an assessment of the quality of atmospheric models and climate runs can be made with respect to the frequency of occurrence and the characteristics of LLJs. When a model simulates the climatology of the nocturnal LLJ in a proper way, it is likely that its representation of the SBL structure is realistic as well. Often model evaluation is based on ''ideal'' case studies, which do not assess the model performance in operational practice. The availability of long-term observations makes the Cabauw site well suitable for deriving climatological information (Van Ulden and Wieringa 1996). Other studies that provide LLJ climatologies are Kurzeja et al. (1991), Whiteman et al. (1997), and Song et al. (2005).

To get insight into the LLJ characteristics at Cabauw, we analyze 7 yr of half-hourly tower and wind profiler observations. Given our extended dataset, we are able to refine our statistics by defining classes that characterize different SBL regimes. This gives valuable insight into how LLJ characteristics depend on different forcing conditions. The development of the LLJ is closely related to the structure of the SBL. For example, according to Blackadar (1957), LLJs often form on top of the nocturnal inversion. Banta et al. (2006) show that the shape of the wind profile depends on stability. The structure of the SBL is determined by a number of factors. In general, the two dominating forcing parameters are radiative cooling and the geostrophic wind speed. The former is mainly determined by the cloudiness and the surface characteristics (soil type and vegetation), while the latter is determined by the horizontal pressure gradient. We classify our data to radiative cooling and geostrophic wind speed. As such, we obtain classes of varying stability, ranging from high wind speed and clouds (deep SBL, weakly stable) to clear sky and calm conditions (shallow SBL, very stable; cf. Mahrt et al. 1998). It will be shown that this classification spans a wide range of SBL wind and temperature structures. For each combination of nocturnal cooling and geostrophic wind, LLJ characteristics are presented. Other parameters that play a role in determining the structure of the SBL are the stability of the residual layer, (shallow) baroclinicity, and large-scale advection. In coastal areas differential heating may play a role. The turbulent structure of the preceding daytime convective boundary layer (CBL) is of influence, as well. The effect of some of these factors on our results will be discussed. To illustrate how our results can be applied for model evaluation, we perform a similar analysis to the 40-yr European Centre for Medium-Range Weather Forecasts (ECMWF) Re-Analysis (ERA-40) data and then compare with the observed climatology.

Section 2 discusses various forcing mechanism of the LLJ. In section 3 the Cabauw site is introduced and we will discuss the observations, while in section 4 we explain how we define an LLJ. Section 5 explains the classification of different types of SBLs in more detail. Next, in section 6, the results are presented. In section 7, a comparison is made with LLJ characteristics in ERA-40. The conclusions are summarized in section 8.

2. Mechanisms

LLJs can be formed by a variety of mechanisms (e.g., Stull 1988; Stensrud 1996). Blackadar (1957) suggested that the diurnal variation in the eddy viscosity leads to nocturnal LLJ formation. When around sunset stable stratification develops, turbulence dies out, and the upper part of the former mixed layer becomes decoupled from the surface. In this layer, where friction does not play a role anymore, the daytime balance of forces is disturbed. As a consequence, the Coriolis force induces an oscillation in the wind vector around the geostrophic wind, producing a supergeostrophic LLJ later during the night. In fact, it is the ageostrophic component of the wind vector at the moment of decoupling that rotates around the geostrophic wind. Figure 1 presents three hodographs of the 200-m winds for selected LLJ cases at Cabauw, in which a clear inertial oscillation is seen. At Cabauw the inertial period amounts to 15.2 h. Note that of course not all LLJs show such a nice development. When, for example, the decoupling is not complete [e.g., for cases with weaker stratification, as shown by Wippermann (1973)] or when mesoscale phenomena (e.g., waves) play a role, this idealized picture will be disturbed.

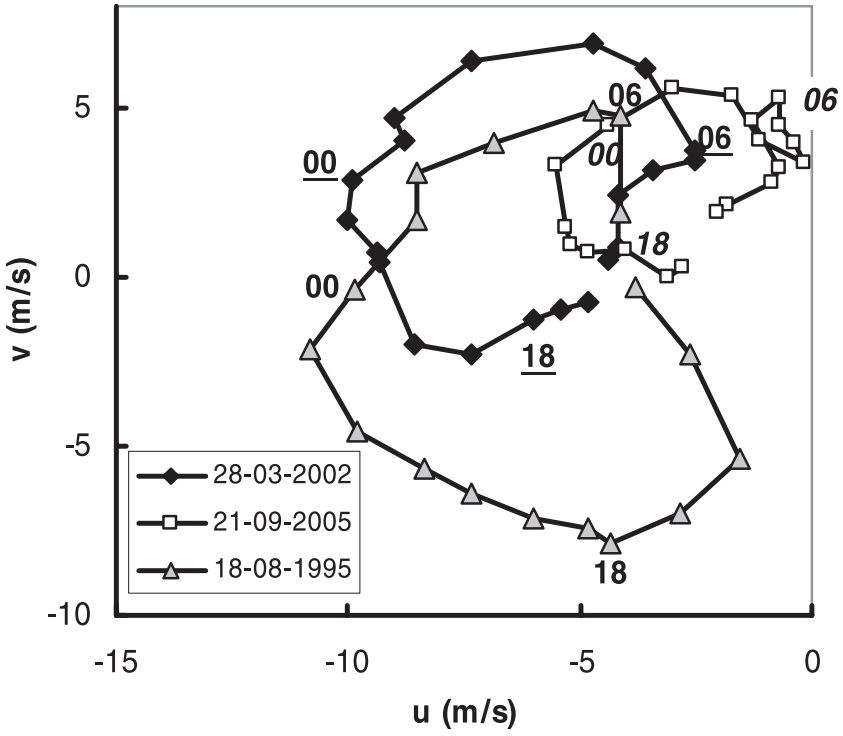

FIG. 1. Hodographs for three nights in which a typical inertial oscillation LLJ occurred. Hourly observations are from Cabauw (200 m). The numbers indicate time in UTC.

Thorpe and Guymer (1977) quantify Blackadar's hypothesis by presenting a simple two-layer bulk model. In this model, the upper layer is frictionless and exhibits an inertial oscillation, while the lower layer is coupled to the surface by momentum exchange. By using this model, Andreas et al. (2000) can explain jet properties as observed above the Antarctic Weddell Sea.

Lundquist (2003) questions the evening-transition hypothesis by stating that the predicted inertial oscillations are rarely observed with satisfying agreement. Chimonas (2005) argues that the period of the observed oscillation is shorter than the true inertial period through the influence of the secondary circulation (i.e., the exchange of air between the boundary layer and the free atmosphere). Besides the collapse of turbulent mixing during the evening transition, frictional decoupling of the flow may also occur when relatively warm air flows out over much colder water (Smedman et al. 1993).

Another mechanism for LLJ formation is large-scale baroclinicity, which may occur for instance near extratropical cyclones (Kotroni and Lagouvardos 1993). When the geostrophic wind speed decreases strongly with height, a low-level wind maximum is likely to occur since close to the ground the wind is retarded by frictional forces. In this case, nocturnal LLJs will show a sharper wind maximum than in barotropic conditions (Blackadar 1957; Wippermann 1973). In regions where significant changes in surface characteristics occur, for example in coastal areas, differential heating may cause shallow baroclinicity, which may produce strong LLJs. Above slightly sloping terrain a diurnal cycle in the horizontal temperature gradient can occur, which may also cause LLJs to develop (Holton 1967).

In their study on the Great Plains LLJ, Whiteman et al. (1997) distinguish between northerly jets related to the passage of cold fronts on the one hand and southerly jets related to an inertial oscillation and the diurnal cycle in horizontal pressure gradient due to sloping terrain on the other hand. This shows that often multiple processes contribute to jet formation (for more examples see Garratt 1985; Banta et al. 2002).

Since the Cabauw site is on flat terrain, we anticipate that frictional decoupling during the evening transition with a subsequent inertial oscillation and baroclinicity due to synoptic systems are the main LLJ forcing mechanisms. Inevitably, the proximity of the North Sea [50 km to the west-northwest (WNW)] plays a role as well. During the summer months the average horizontal pressure gradient (or geostrophic wind) near the surface shows a clear diurnal cycle: after 1000 UTC the dominating geostrophic wind direction starts to veer from

WSW to NE directions (see Van Delden 1993). This corresponds to relatively high pressure above the sea and low pressure above land, which is caused by differential heating. After 1900 UTC, which is around sunset, the average geostrophic wind direction becomes WSW again. Therefore, LLJs related to the passage of a sea-breeze front will weaken after sunset. Since we are mostly interested in LLJs at 6 h after sunset we expect that the influence of sea-breeze–induced LLJs on our results is relatively small. Nevertheless, it is likely that the diurnal variation in the horizontal pressure gradient influences the ageostrophic wind component in the afternoon and therefore determines how the inertial oscillation develops. We note that no sea-breeze circulation develops when the opposing (i.e., easterly) flow is stronger than 5 m s^{-1} (Tijm et al. 1999).

3. Site characteristics and observations

The Cabauw measuring site is situated in the western part of the Netherlands (51.971°N, 4.927°E) in topographically flat terrain. The distance to the North Sea is about 50 km in the WNW direction. The climate is maritime with rainfall in every season. Southwesterly winds predominate, especially during winter. In the summer half-year the winds are more equally distributed among the compass rose. The majority of geostrophic winds of more than 20 m s^{-1} occur for southwesterly flow in winter. The area around the site consists of meadows, fields, and scattered villages. The roughness length varies with wind direction (see Verkaik and Holtslag 2007). The terrain around the 200-m main tower is free from obstacles up to a few hundred meters in all directions. More details and site characteristics can be found in Van Ulden and Wieringa (1996) and Beljaars and Bosveld (1997).

In this study we use 7 yr of half-hourly wind observations (1995, 1996, and 2001–05) from the 200-m mast and a 1290-MHz wind profiler/radio acoustic sounding system (RASS). (The wind profiler became operational in 1994, and between 1996 and 2001 no regular tower observations are available.) On the mast, wind speed and wind direction are measured at 10, 20, 40, 80, 140, and 200 m with propeller vanes (1995, 1996) and cup anemometers (2001–05). The accuracy of the propeller vanes and the cup anemometers is better than 0.5 m s^{-1}. For different heights, both instruments show a similar probability density function of the wind speed. Availability of the mast measurements is close to 100%.

The wind profiler is situated 300 m south of the main tower. For this instrument, wind speed and direction are retrieved with a vertical sampling interval of 60 m. The retrieved values consist of range-weighted averages over layers of approximately 100 m. For this study we use data from 200 up to 1420 m. Specifications of the profiler can be found in Klein Baltink (1998). Unfortunately, the radar reflections from the rotating cup anemometers in the mast contaminated the signal of the wind profiler in the range of 300–430 m above ground level for extended periods of time from 2001 onward. By applying a more advanced postprocessing technique, the so-called multiple peak processing algorithm (see, e.g., Gaffard et al. 2006), we strongly reduced this problem. For the wind profiler, data availability depends, among other things, on the atmospheric conditions. For weakly stable conditions the availability decreases steadily with height from about 80% at 200 m to about 50% at 1400 m. With increasing stability, the availability decreases to values of 80% at 200 m and 30% at 1400 m for very stable conditions. (Here ''weakly stable'' and ''very stable'' refer to the two extreme classes in our classification described in section 5 with the highest/lowest geostrophic forcing and lowest/highest nocturnal cooling, respectively.) Missing values were filled in by linear interpolation, but only if not more than two consecutive observations were lacking.

Extra attention has to be paid to the transition between the mast and the wind profiler. An intercomparison of 2 yr of wind observations at 140 and 200 m above ground level showed good agreement between the two systems (Klein Baltink 1998). However, the detection of LLJs is based on gradients in the wind profile and is therefore sensitive to small differences between the mast and the wind profiler. For this reason, we discarded profiles for which at 200 m this discrepancy is more than 2 m s^{-1}. If the difference is less than 2 m s^{-1}, the complete profile of the wind profiler is shifted to the mast 200-m winds to eliminate the remaining difference. In this way the shape of the profiles of both the tower and the wind profiler remains intact. These procedures guarantee a smooth transition between the mast and the profiler.

Besides the wind observations described above, auxiliary data from other instruments are used. Geostrophic winds are derived from a planar fit of pressure observations from eight synoptic weather stations in a radius of 75 km around Cabauw. Profiles of virtual temperature T_v, which are used to estimate the inversion height, are derived from the wind profiler/RASS. Below 200 m, this quantity is derived from observations of air temperature T_a and relative humidity RH, measured by Pt500-elements and Vaisala HMP243 heated relative humidity sensors, respectively (at similar levels as the wind observations). The virtual temperature is calculated by

$$T_v = T_a(1 + 0.61r), \tag{1}$$

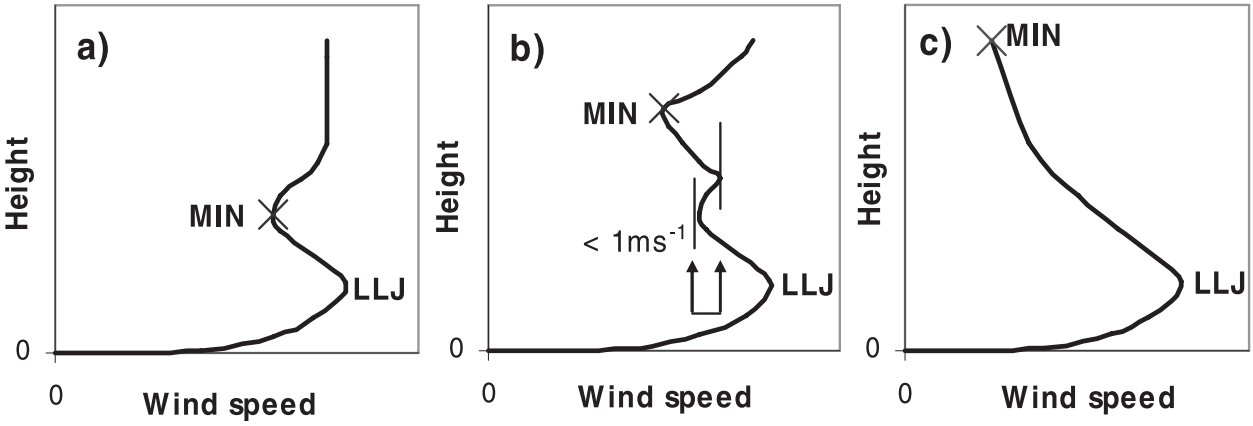

FIG. 2. Illustration of the detection of LLJs. (a) An LLJ is defined as a maximum in the wind speed profile that is 2 m s^{-1} and 25% faster than the next minimum above. (b) A minimum is neglected if the wind speed above increases less than 1 m s^{-1} before decreasing again below the minimum. (c) If no minimum is present the lowest wind speed in the profile is taken as a minimum.

where r is the mixing ratio. Note that the RASS detects the acoustic virtual temperature, which differs slightly from the buoyancy virtual temperature, as defined by Eq. (1) (Kaimal and Gaynor 1991). For our purpose this difference can be neglected. The incoming longwave radiation $L^{\downarrow}$, used to calculate the isothermal net radiation (see section 5), is measured with an Eppley pyrgeometer. If data from this instrument are missing, data from a Schulze radiometer are used instead.

4. Criteria for LLJ detection

In the literature many different criteria for LLJs are applied. Following Stull (1988), Andreas et al. (2000) define an LLJ as a maximum in the vertical profile of the wind speed that is at least 2 m s^{-1} faster than wind speeds above and below it within the lowest 1500 m of the atmosphere. Banta et al. (2002) apply a comparable criterion, but with a threshold value of (in specific cases) only 0.5 m s^{-1}. Instead of a fixed threshold value, a relative value can be used by, for example, requiring a falloff of 20% relative to the wind maximum. Bonner (1968) introduces classes of different types of LLJs by defining threshold values for both the speed of the LLJ and the required falloff above the jet. This classification was adopted by Whiteman et al. (1997).

In this study we define an LLJ as the lowest maximum of the wind speed profile in the lowest 500 m of the atmosphere that is at least both 2 m s^{-1} *and* 25% faster (equivalent to a 20% falloff) than the next minimum above (Fig. 2a). The absolute criterion prevents that in very calm conditions small variations in the wind profile (in the order of measuring errors) are classified as a low-level jet. The relative criterion does the same in cases of high wind speed, where the 2 m s^{-1} criterion may be accidentally satisfied. A minimum is neglected if the wind speed above that minimum increases less than 1 m s^{-1} before decreasing again to values lower than the wind speed of that minimum. Instead, a minimum higher up is chosen (Fig. 2b). When no minimum is present (so the wind speed decreases constantly above the maximum) the lowest value of the wind speed profile above the jet is taken as a minimum (Fig. 2c).

A wind profile is only classified as an LLJ if the two neighboring half-hour records satisfy the criteria for an LLJ as well. This is done to guarantee that the detected jets show some persistence in time. We acknowledge that these criteria—as any others—are subjective. To assess the influence of the required falloff, for some cases we compare our results with definitions applied in other studies.

Our analysis focuses on the first 6 h of SBL development (see section 5). For each night, we analyze the wind profile at 6 h after sunset. To not be too dependent on the availability and quality of this particular profile, the (half-hourly) wind speed profiles from 5 to 7 h after sunset are analyzed. When multiple profiles contain an LLJ, the one closest to 6 h after sunset is included in the statistics. If no LLJ is detected, the night is classified as a non-LLJ night.

Because, in principle, LLJs caused by large-scale baroclinicity are not related to the boundary layer structure, we experimented with criteria to exclude cases for which the geostrophic wind decreased substantially with height. The geostrophic wind speed at the surface was estimated from surface pressure observations from a network of synoptic stations around Cabauw. At 1500 m we used the ordinary wind from the

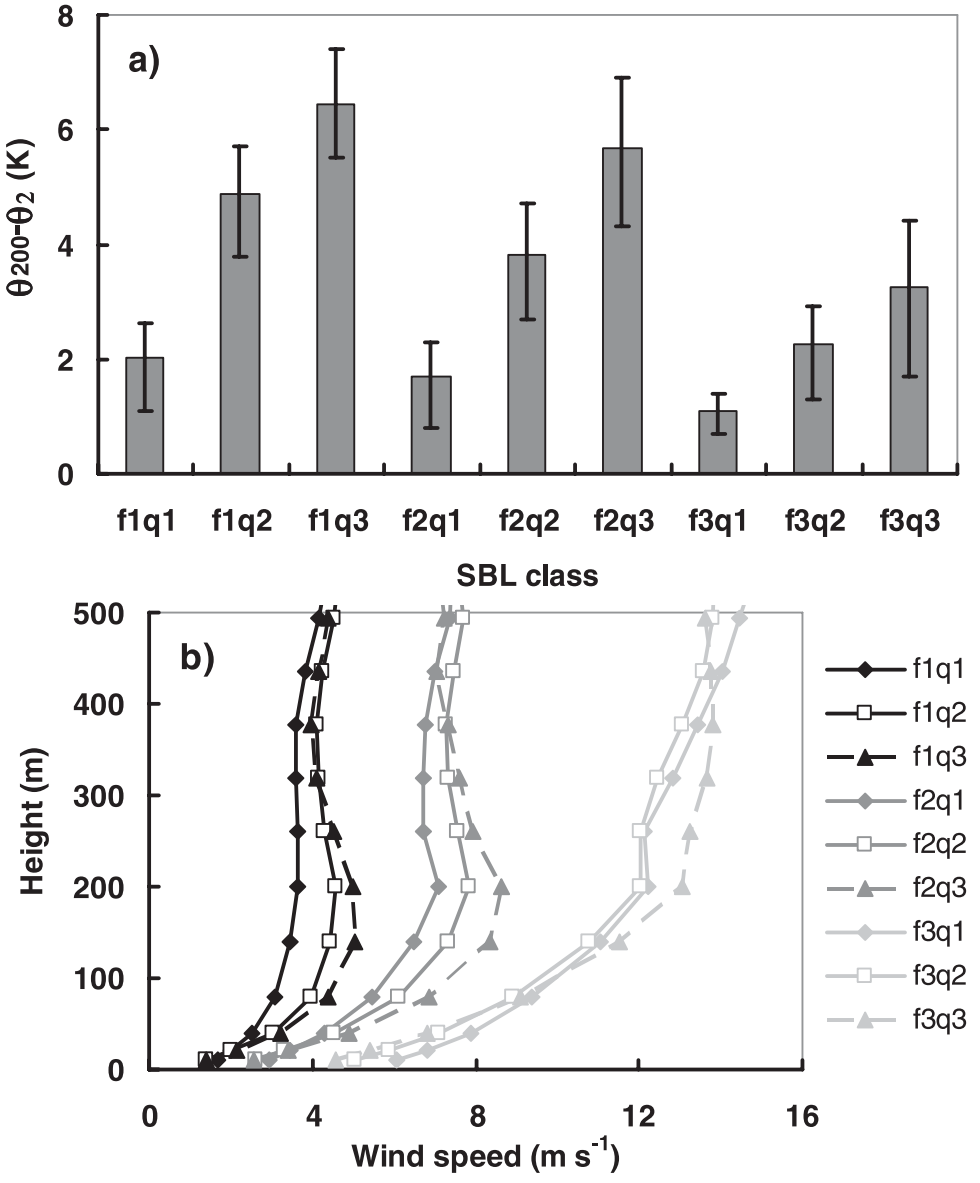

FIG. 3. (a) Average inversion strength, expressed as the potential temperature difference between 200 and 2 m, $\theta_{200} - \theta_2$, for different classes of SBLs. Error bars indicate the 0.25 and the 0.75 percentiles. (b) Average wind profiles for the nine SBL classes. Only data 6 h after sunset are used. Here, f1, f2, and f3 correspond to $V_g \leq 5$ m s^{-1}, $5 < V_g \leq 10$ m s^{-1}, and $V_g > 10$ m s^{-1}, and q1, q2, and q3 correspond to $\Delta T_{\text{iso}} \leq 3$ K, $3 < \Delta T_{\text{iso}} \leq 6$ K, and $\Delta T_{\text{iso}} > 6$ K.

ERA-40 database (operational ECMWF output was used after August 2002 when ERA-40 ended) as a proxy for the geostrophic wind, since the latter is not available in the ERA-40/ECMWF output. If this estimate is more than 5 m s^{-1} lower than the geostrophic wind at the surface, the wind profile is considered baroclinic and occurring jets are not included in the statistics.

To test whether the assumption that the ordinary wind can be used instead of the geostrophic wind is realistic, we made use of a 2-yr run (2002 and 2003) of the Regional Atmospheric Climate Model (RACMO) in operation at the Royal Netherlands Meteorological Institute (KNMI). For this run the geostrophic winds were archived. Every day the model is run from the ECMWF analysis. Comparison of the ordinary and geostrophic winds within RACMO at about 1500 m showed a bias of only 0.1 m s^{-1} and a standard deviation of 1.6 m s^{-1}. These small deviations justify our assumption of using the ordinary wind as a proxy for the geostrophic wind.

5. Classifying SBL observations

The LLJ characteristics presented in section 6b are classified to different types of SBLs in a way that is similar to that done by Bosveld and Beyrich (2004). The classification is based on two external forcing parameters, which in general determine the development of the SBL. These are the surface geostrophic wind speed and the nocturnal radiative cooling. [Note that Bosveld and Beyrich (2004) used the 200-m wind as a proxy for the geostrophic wind.] The advantage of using external parameters is that these do not depend on the development of the SBL itself (Van de Wiel et al. 2002). For example, as a measure of the cooling the net radiation at the surface could be used. However, this quantity is influenced by local thermal characteristics of the surface and depends on the structure of the SBL. Instead, we prefer to use the so-called isothermal net radiation at the top of the SBL (Monteith 1981; Holtslag and de Bruin 1988). Since the temperature at the top of the SBL is not readily available, we use the temperature at 200-m height as a proxy. Thus, we define the isothermal net radiation Q_i^* as

$$Q_i^* = L^{\downarrow} - \varepsilon_s \sigma (T_{a200})^4, \tag{2}$$

where $L^{\downarrow}$ is the incoming longwave radiation, T_{a200} is the air temperature at 200 m, σ is the Stefan–Bolzmann constant, and ε_s is the emissivity of the surface. For grass a good approximation of ε_s is 1 (Holtslag and de Bruin 1988), a value that is adopted in this study.

We focus on the SBL development in the first 6 h after sunset. Although the inertial oscillation amounts to 15.2 h, nocturnal LLJs should reach their maximum speed around 6 h after sunset. First, the wind vector at the moment of decoupling is already veered compared to the geostrophic wind. Second, the transition to stable stratification occurs often well before sunset. We define three classes for the average geostrophic wind speed V_g over the first 6 h of the night: $V_g \leq 5$ m s^{-1}, $5 < V_g \leq 10$ m s^{-1}, and $V_g > 10$ m s^{-1}. For the isothermal longwave radiative cooling three classes are defined as well: $\Delta T_{\rm iso} \leq 3$ K, $3 < \Delta T_{\rm iso} \leq 6$ K, and $\Delta T_{\rm iso} > 6$ K. Here $\Delta T_{\rm iso}$ is the temperature drop that the net isothermal longwave cooling, integrated over the first 6 h after sunset, would cause in a 200-m-high column of air:

$$\Delta T_{\rm iso} = -\frac{1}{200} \sum_{t=0}^{6\,\rm h} \frac{Q_i^*(t)}{\rho c_p}, \tag{3}$$

where ρ is the density of air (taken as 1.2 kg m^{-3}) and c_p is the specific heat capacity of air. Note that each 1-K temperature drop corresponds to a radiative cooling of 12 W m^{-2}.

TABLE 1. Distribution of nights over classes of SBL. The top numbers indicate the total number of nights for each class. The lower numbers, in italic, indicate the percentage of occurrence for each class in winter (October–March) and summer (April–September). For example, 154 nights are classified in the class with high geostrophic forcing and intermediate nocturnal cooling. In winter, 16% of the nights fall into this class; in summer, 8%.

	$V_g \leq 5$	$5 < V_g \leq 10$	$V_g > 10$	Total
$\Delta T_{\rm iso} \leq 3$	70	191	232	493
	6 | 5	*15 | 14*	*26 | 11*	
$3 < \Delta T_{\rm iso} \leq 6$	121	180	154	455
	2 | 14	*11 | 15*	*16 | 8*	
$\Delta T_{\rm iso} > 6$	109	174	106	389
	3 | 12	*10 | 15*	*11 | 6*	
Total	300	545	492	1337

Combining the classes of geostrophic wind speed and isothermal cooling yields nine classes in total. Each of them represents a different SBL structure. This is illustrated in Fig. 3. Figure 3a shows the average inversion strength, expressed as the potential temperature difference between 200 and 2 m, $\theta_{200} - \theta_2$, for each class. Values vary from about 1 to 6 K and the error bars (which indicate 0.25 and 0.75 percentiles) are small. The average wind profiles are given in Fig. 3b. When $V_g < 10$ m s^{-1}, the wind speed increases for increasing nocturnal cooling. Except for the class with the strongest V_g, even the average wind speed profiles show a low-level maximum. Figure 3 demonstrates that our classification covers a wide range of SBLs in both wind and temperature structures.

Of the total of 2553 nights considered, 2270 could successfully be classified into one of the defined classes. After we rejected all profiles for which the difference in wind speed at 200 m between the mast and the wind profiler exceeded 2 m s^{-1} and for which more than two consecutive observations in the lowest 500 m were missing, 1337 nights remained. The number of nights in each class combination is listed in Table 1, together with the frequency of occurrence of each class in both summer and winter.

6. Climatology of LLJs

In section 6a some general characteristics of LLJs at Cabauw are discussed. Except for the analysis of the diurnal cycle, for each night only the profile around 6 h after sunset is analyzed, as explained in section 4. Section 6b presents the results for the classification into different SBL types. A comparison with model output is made in section 6c.

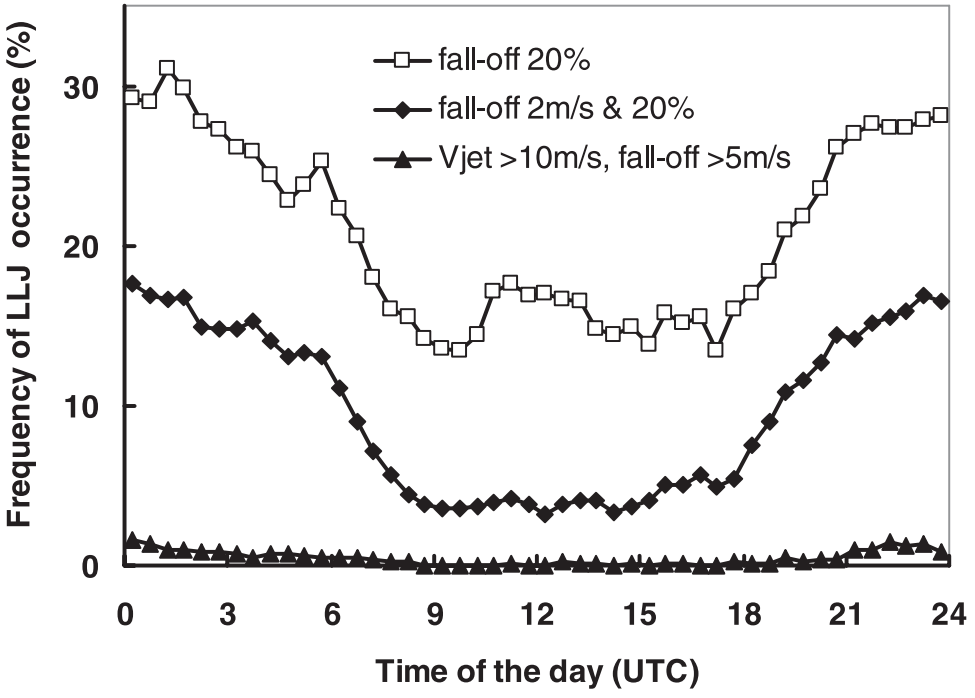

FIG. 4. Diurnal variation of LLJ occurrence for different definitions of the LLJ.

a. General characteristics

Van Ulden and Wieringa (1996) mention that at Cabauw, nocturnal LLJs are a commonly occurring phenomenon. This is confirmed by Fig. 4, which shows a clear diurnal cycle in LLJ occurrence. At night, the wind speed profile satisfies our criteria (the thick solid line with diamonds) for an LLJ in almost 20% of the nights. During daytime the frequency of occurrence is much lower, on the order of 3%–4%.

For comparison the results for some other definitions are added. It appears that the results depend considerably on the choice of the definition. When only a 20% falloff is required, many more LLJs are detected. However, most of the extra jets are very weak so that it is questionable whether they can be considered LLJs. Moreover, the difference between the speed of the jet and the minimum above becomes about 1 m s^{-1}, which is on the order of the accuracy of the instruments (i.e., the wind profiler). For wind energy applications, aviation, or SBL dynamics, these minor ''jets'' are probably not important. Figure 4 also shows the occurrence of LLJs of more than 10 m s^{-1}, with a decrease of at least 5 m s^{-1} aloft. This criterion was used by Bonner (1968) and more recently by Whiteman et al. (1997) and Song et al. (2005) for the Great Plains jet. Apparently, this type of jet is much rarer at Cabauw. For example, compare Fig. 4 with Whiteman et al.'s (1997) Fig. 3.

Many studies highlight the role of the large-scale sloping terrain, which would enhance the Great Plains LLJ (e.g., Holton 1967; McNider and Pielke 1981). This could be used as an argument to explain differences between the LLJs of the Great Plains and of Cabauw, as was suggested by Van Ulden and Wieringa (1996). However, other studies show that the effect of the sloping terrain is of much less importance than the inertial oscillation (Parish et al. 1988), while the study of Jiang

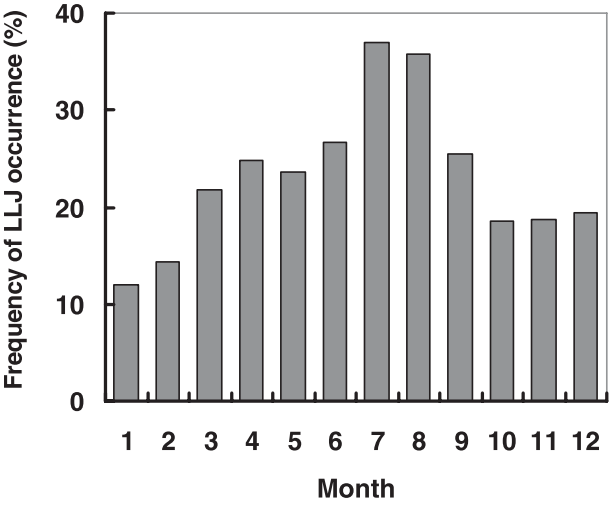

FIG. 5. Frequency of occurrence of LLJ nights per month.

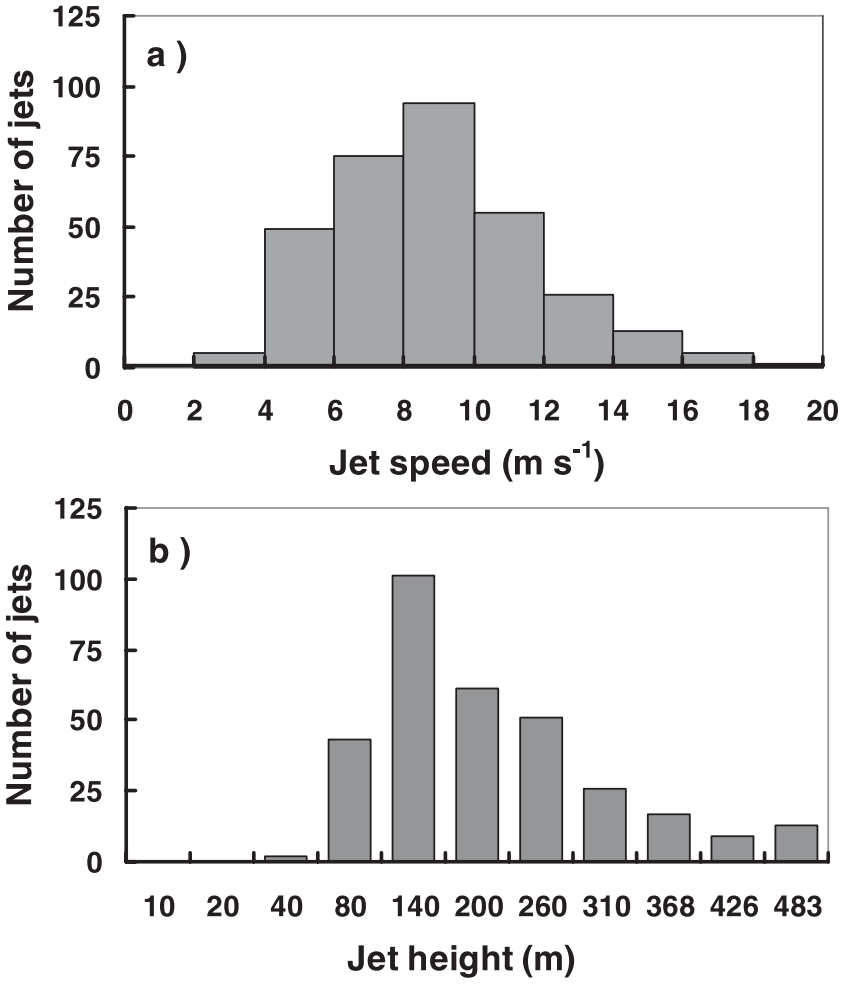

FIG. 6. Frequency distribution of LLJ (a) speed and (b) height, based on LLJs 6 h after sunset.

et al. (2007) concludes that both mechanisms are of equal importance. Apart from possible effects of sloping terrain on the Great Plains LLJ strength, we suggest that the discrepancy between LLJs at Cabauw and the Great Plains can also be explained by differences in the turbulent structure of the daytime convective boundary layer. In the Great Plains, turbulence is probably much more vigorous, for example, because the Bowen ratio is much higher than 0.25, which is typically observed in Cabauw. More intensive turbulence results in larger ageostrophic wind components. As a result, stronger LLJs will occur. This agrees with the findings of Zhong et al. (1996), who conclude that drier soils enhance the amplitude of the diurnal oscillation in the wind. Note also that differences in study objectives and therefore in the definition of the LLJ, as well as the use of different instrumentation, can cause differences in LLJ statistics (Banta et al. 2002).

Figure 5 presents the seasonal cycle of LLJs. Clearly, LLJs occur most often in the summer months. This can be explained by two reasons. First, in summer the daytime boundary layer is much more convective than in winter. More vigorous turbulence is associated with larger ageostrophic wind components. As a result, nocturnal inertial oscillations will show larger amplitude than in winter. Thus, in summer it is the stronger coupling between the boundary layer and the earth's surface that stimulates the formation of nocturnal LLJs (e.g., Wilczak et al. 1997). Second, in winter the frequency of cloudy nights with strong geostrophic forcing is much higher than in summer (see Table 1). In section 6b it will be shown that for these conditions LLJ occurrence is low.

The distribution of LLJ speeds is given in Fig. 6a, while Fig. 6b presents the distribution of LLJ heights (based on one observation per night, 6 h after sunset). It

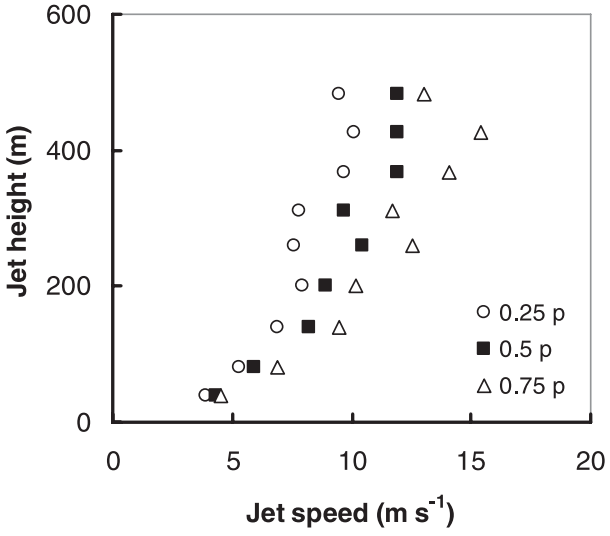

FIG. 7. Relation between LLJ height and LLJ speed. The black squares indicate the medians. As a measure for the spread, the 0.25 and 0.75 percentiles are given. (Based on LLJs 6 h after sunset.)

appears that at Cabauw, LLJs typically have a moderate speed of 6–10 m s^{-1} and are located 140–260 m above the surface. These numbers compare well to values presented by Banta et al. (2002) and Andreas et al. (2000), for the Cooperative Atmospheric–Surface Exchange Study 1999 (CASES99) and the Ice Station Weddell (Antarctica) dataset, respectively. The same is true for the Stable Atmospheric Boundary-Layer Experiment in Spain (SABLES; Conangla and Cuxart 2006). Plotting the LLJ height versus the speed of the LLJ (Fig. 7) shows a tendency for stronger LLJs to occur at higher levels. Banta et al. (2002) found similar results for the CASES99 dataset (their Fig. 6).

To investigate whether any preferred directions of the large-scale flow exist for LLJ formation, Fig. 8a shows how the nocturnal jets at Cabauw are distributed over classes of geostrophic wind direction (45° increments). The different areas represent different classes of geostrophic wind speed. The distribution shows a broad peak for easterly directions (45°–180°). Another peak in the LLJ occurrence occurs for WSW directions (225°–270°) of the large-scale flow. Figure 8b explains this distribution. It shows the climatological distribution of the direction of V_g. The average value of ΔT_{iso} for each class of geostrophic wind direction is also presented. Probably, the peak in LLJ occurrence for WSW directions is associated with the dominance of this direction in the total wind distribution. The peak in LLJ occurrence for easterly directions, as observed in Fig. 8a, can be related to a maximum in the radiative cooling, which is given in Fig. 8b. The low number of LLJs for northerly directions is likely to be related to the relatively low cooling values. The minimum in the ΔT_{iso} is associated with the presence of the North Sea. For westerly winds (from the coast), on average cloud cover is higher, which leads to lower nocturnal cooling rates than for easterly, more continental air masses. LLJs associated with strong geostrophic forcing are most frequent for the WSW direction. The division into classes of V_g shows that for strong geostrophic forcing LLJ occurrence is less likely than for low or moderate geostrophic forcing.

We also investigated the relation between the height of the LLJ and the height of the nocturnal temperature inversion. The inversion top is defined as the height of the lowest (virtual) temperature maximum above the surface. Figure 9 shows that in most cases the LLJ is situated close to the top of the inversion layer, which is consistent with the inertial oscillation hypothesis of Blackadar (1957). For southerly LLJs in the Great Plains region, Bonner (1968) and Whiteman et al. (1997) find that the jet heights are generally above the tops of the nocturnal inversions (with large variability from case to case). Andreas et al. (2000) find that most LLJs above the Antarctic Weddell Sea, most likely caused by inertial oscillations, are embedded in the inversion layer.

b. *Classification into SBL types*

Figure 10 gives LLJ characteristics for the nine classes of SBLs defined in section 5. The labels f1, f2, and f3 in Fig. 9 indicate increasing V_g, while q1, q2, and q3 indicate increasing longwave cooling. The frequency of occurrence of LLJs is shown in Fig. 10a. Apparently, strong nocturnal cooling facilitates LLJ formation. This is the case for all three classes of geostrophic wind. For strong geostrophic forcing, the occurrence of LLJs is strongly decreased relative to moderate and weak geostrophic forcing. These results suggest that frictional decoupling after sunset is an important forcing mechanism of the Cabauw LLJ. At low cooling rates (e.g., caused by the presence of clouds), the stable stratification is weak (see, e.g., Fig. 3a). It is likely that in this case decoupling of the SBL will not occur or only to some degree. As a result, acceleration of the flow through inertial forces is strongly reduced or inhibited and no LLJ will be formed. Comparably, for high geostrophic forcing turbulent mixing maintains the coupling between the surface and the layers aloft, explaining the low frequency of nocturnal LLJ occurrence in these classes. Contrary to what is observed, one would expect the highest frequency of occurrence for the lowest wind class, because then the stable stratification is maximized (see Fig. 3a). However, for these calm conditions the wind maxima are often so weak that they do not pass the

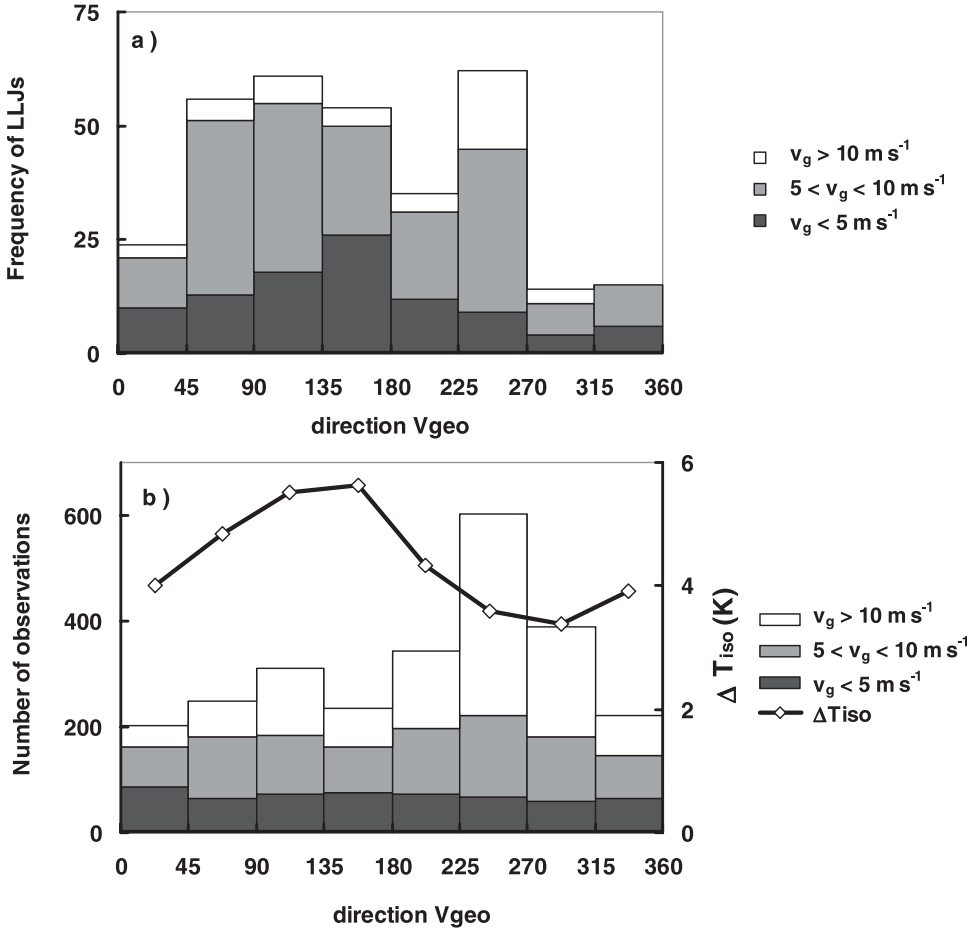

FIG. 8. (a) Distribution of LLJ occurrence for classes of the geostrophic wind direction. (b) The climatological distribution of the geostrophic wind direction. The solid line in (b) indicates the average value of the isothermal net radiative cooling for each class of geostrophic wind direction.

2 m s^{-1} falloff criterion. We suppose that in this case the ageostrophic wind component is too small to produce a significant inertial oscillation [see also Rama Krishna et al. (2003)]. If we would apply only the 20% falloff criterion, the lowest wind class *would* show the highest frequency of occurrence.

In Fig. 10b the average height of the LLJs is shown for each class. For decreasing geostrophic forcing the LLJs are located at a lower altitude. This was also found by Rama Krishna et al. (2003). The LLJ height increases with decreasing radiative cooling. The height varies from about 130 m for the most stable class to about 300 m for the class with the weakest stability. This tendency agrees with the theoretical concept that the jets form at the top of the SBL, which is shallower for strong nocturnal cooling rates and low geostrophic forcing.

The turning of the wind vector between the jet nose and the wind measured at 10 m above ground level (Fig. 10c) increases with increasing cooling, except for the highest wind class. However, the dependency on the geostrophic forcing seems to be small. On average, the turning angle between the jet nose and the surface is close to 35°, a value that was earlier reported for clear sky nocturnal boundary layers at Cabauw by Van Ulden and Holtslag (1985). Assuming that the LLJ height is closely related to the nocturnal boundary layer height, Figs. 10b and 10c also support the conclusions of Svensson and Holtslag (2009) that deeper (shallower) boundary layers exhibit smaller (larger) turning of the wind vector with height: going from q1 to q3 the LLJ is situated at lower altitudes (Fig. 10b), while (except for the highest wind class) the turning increases (Fig. 10c).

Concerning the speed of the LLJs, Fig. 10d shows that supergeostrophic jets are most common for $V_g \leq 5$ m s^{-1}. Except for the lowest geostrophic wind class, there is a small tendency for the speed of the LLJs to increase for higher values of the nocturnal cooling. It should be noted that contrary to Fig. 10a, for Figs. 10b–d

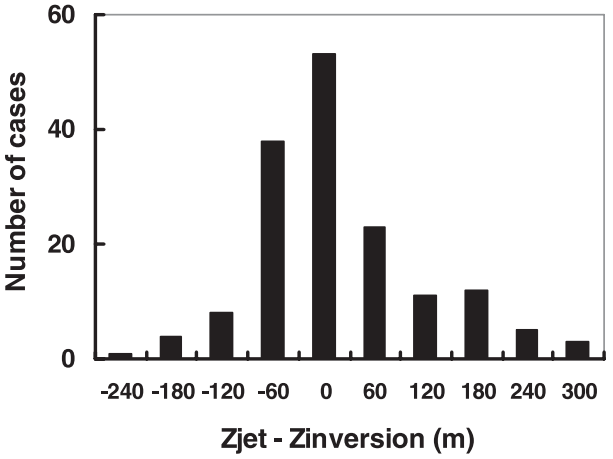

FIG. 9. Difference in height between the LLJ and the virtual temperature inversion.

the results are not sensitive to the choice of LLJ definition (not shown).

So far the results can be well interpreted within the context of Blackadar's inertial oscillation theory of LLJ formation. This suggests that frictional decoupling around sunset is the main mechanism for LLJ formation at Cabauw. However, one might ask whether or not a more detailed selection can be made, which focuses on some conceptual characteristics of the inertial oscillation (see, e.g., Beyrich 1994). As such, we applied additional selection criteria by only selecting LLJs for which the jet speed is supergeostrophic and for which the wind vector veers from 5 to 7 h after sunset. Thus, we select only jets that show clear features of an inertial oscillation. About 60% of all LLJs satisfy these criteria. However, the characteristics of these jets (in terms of height and turning compared to the 10-m wind) do not differ from those of the remaining 40% of the LLJs. This suggests that also in the formation of the latter, frictional decoupling after sunset plays a role. In summer the fraction of LLJs with clear inertial oscillation characteristics is twice as large as in winter.

7. Comparison with ERA-40 climatology

Above we presented climatological characteristics of the LLJ with the objective of facilitating the evaluation of atmospheric models. As a proof of principle, we now show how a comparison between our results and an atmospheric model can be performed. We use hourly output from ERA-40 (Uppala et al. 2005), in particular from the grid point closest to Cabauw. This is the first complete land grid point, next to the North Sea. The resolution is T157 with 60 vertical levels. The lowest model levels are at 10, 30, 70, 120, and 190 m. The surface characteristics in the model are representative of the central parts of the Netherlands. Bosveld and Beyrich (2004) show that the model is able to capture the basic structures of the SBL at Cabauw. However, they conclude that the vertical gradients of wind and temperature in the model are too weak and that the turning of the wind vector across the SBL is strongly underestimated.

Although in principle we could take any other representative period, for consistency we decided to analyze the same period as covered by the observations (i.e., the years 1995, 1996, and 2001–05). Since the ERA-40 archive runs only to August 2002, we added operational ECMWF output for the remainder of the period. Some model changes occurred during this period, but no significant adjustments took place in the formulation of the stable boundary layer. Analysis of the period 1986–95 (only ERA-40 data) gave similar results.

Because there are no quality issues involved and model output is much smoother than observations, only the profile at 6 h after sunset is analyzed. Like the observations, the model wind profiles were classified following the procedure described in section 5. Ideally, the classification parameters V_g and ΔT_{iso} were both taken from model output. Since V_g is not readily available in ERA-40 we took the value derived from the pressure observation from the synoptic stations. Following Eq. (2), ΔT_{iso} was calculated using $L^{\downarrow}$ and T_a from the model level closest to 200 m.

The ERA-40 LLJ characteristics for Cabauw are given in Fig. 11. The frequency of occurrence of LLJs (Fig. 11a) is much lower in the model than in the observations. However, the tendencies as a result of varying V_g and ΔT_{iso} are clearly present: the number of LLJs increases significantly for increasing nocturnal cooling and for the highest class of V_g the frequency of occurrence is very much decreased. The average height of the LLJ (Fig. 11b) is systematically overestimated by ERA-40 by about 50–100 m (except for the class f1q1). Moreover, in the model the individual jets are much more spread out in height than in the observations: this is expressed in the much higher level of the wind speed minimum above the LLJ (not shown). The turning of the wind vector between the LLJ height and the lowest model level (~10 m) (Fig. 11c) is too low relative to the observed values. Also, the speed of the LLJs is underestimated in the model (Fig. 11d).

To summarize, the frequency of LLJs in ERA-40 is underestimated at Cabauw. The same is true for the turning across the boundary layer and the speed of the jet, while the jet height is overestimated. This is consistent with the results of Bosveld and Beyrich (2004) and agrees with the findings of Cheinet et al. (2005), who attribute this disability to properly represent the LLJ to deficiencies

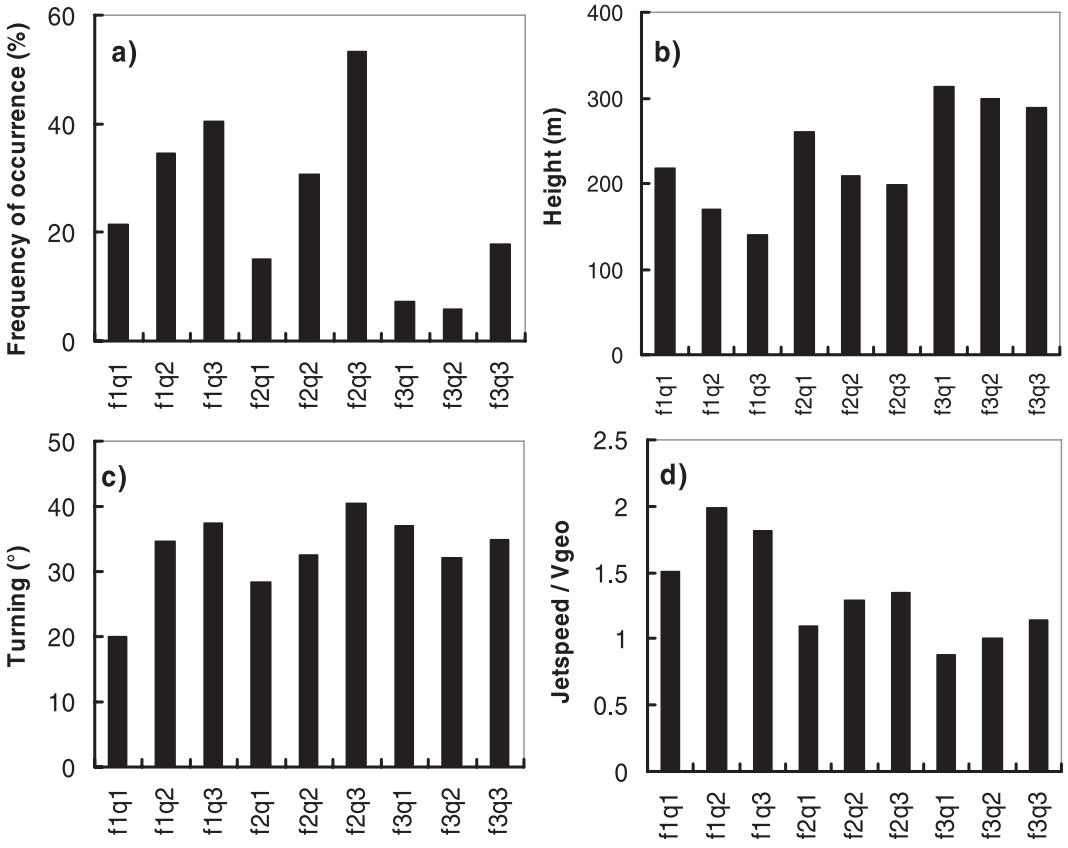

FIG. 10. LLJ characteristics for nine classes of SBLs. (a) Frequency of LLJ occurrence, (b) jet height, (c) turning of the jet relative to the 10-m wind, and (d) jet speed relative to the geostrophic wind. Here, f1, f2, and f3 correspond to $V_g \leq 5$ m s^{-1}, $5 < V_g \leq 10$ m s^{-1}, and $V_g > 10$ m s^{-1}, and q1, q2, and q3 correspond to $\Delta T_{\text{iso}} \leq 3$ K, $3 < \Delta T_{\text{iso}} \leq 6$ K, and $\Delta T_{\text{iso}} > 6$ K.

in the SBL mixing formulation. To obtain optimal model scores on the synoptic scale, the model applies stability functions for vertical diffusion in stable conditions that allow for much more mixing than can be motivated by field experiments. The consequent degradation of the representation of the SBL is taken for granted. Comparable results were found in the first Global Energy and Water Cycle Experiment (GEWEX) Atmospheric Boundary Layers Study (GABLS1) intercomparison on a stably stratified case by Cuxart et al. (2006) and by Baas et al. (2008), who analyzed different parameter settings of a turbulent kinetic energy (TKE) closure model. Since modeling of the LLJ does not seem very sensitive to vertical resolution (Ghan et al. 1996), we expect that the deficiencies in the physical parameterization dominate over possible influences of resolution.

8. Concluding remarks

The main objective of this study was to provide a climatology of low-level jets to facilitate the evaluation of atmospheric models. Therefore, 7 yr of half-hourly observations of wind speed profiles from the Cabauw measuring site in the Netherlands were analyzed. Data from a 1290-MHz wind profiler were used to extend the measurements of a 200-m-high tower to obtain wind and temperature profiles up to 1420 m above ground level. In about 20% of the nights a substantial maximum in the nocturnal wind speed profile occurs. At Cabauw, LLJs typically have a speed of 6–10 m s^{-1} and are situated at 140–260 m. Despite predominant southwesterly wind directions, most LLJs have more easterly–southerly directions. Analysis of vertical profiles of virtual temperature showed that the height of the LLJ is often close to the height of the nocturnal inversion.

Moderate geostrophic forcing and high radiative cooling (no clouds) are the most favorable circumstances for the development of a substantial LLJ. For stronger nocturnal cooling and lower geostrophic forcing, the LLJs form at a lower altitude. The difference in wind direction between the LLJ and the 10-m wind increases for increasing nocturnal cooling. These results

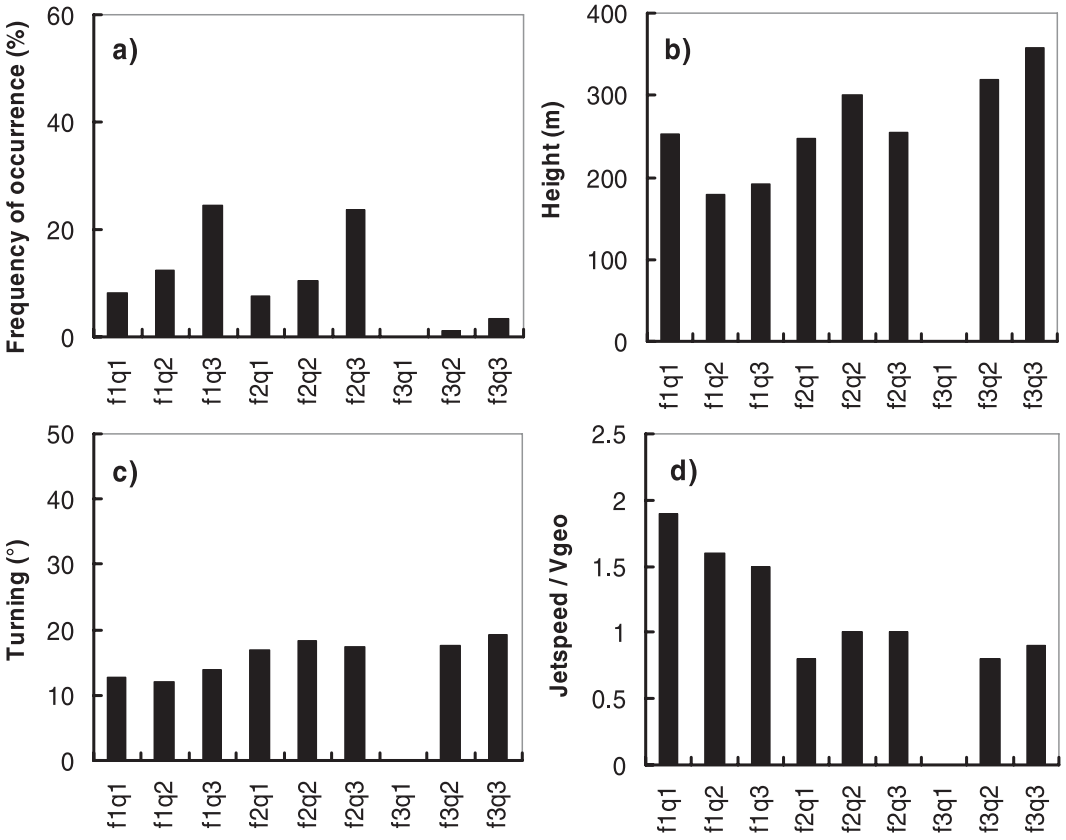

FIG. 11. As in Fig. 10, but for ERA-40 [after the ERA-40 archive ended (August 2002), operational ECMWF output was used].

suggest that frictional decoupling after sunset as a result of stable stratification is the main mechanism for LLJ formation at Cabauw. Indeed, about 60% of the detected LLJs show features of a well-developed inertial oscillation. However, the characteristics of these jets (in terms of height and turning compared to the 10-m wind) do not differ from those of the remaining 40% of the LLJs.

To illustrate the applicability of the derived climatology for model evaluation, we compared some of our results with output from the ERA-40 archive. It appears that LLJs in the model are less frequent and situated at a higher level than in the observations. The turning across the boundary layer is smaller than observed. Also the speed of the LLJ is underestimated.

Acknowledgments. We acknowledge Martin Köhler (ECMWF) for providing operational output from the ECMWF model for the grid point close to Cabauw. Three anonymous reviewers are acknowledged for their constructive comments. The first author has been supported by the Netherlands Organization for Scientific Research (NWO), in particular through the project ''land surface climate and the role of the stable boundary layer.''

REFERENCES

Anderson, C. J., and R. W. Arritt, 2001: Representation of summertime low-level jets in the central United States by the NCEP–NCAR reanalysis. *J. Climate,* **14,** 234–247.

Andreas, E. L, K. J. Claffey, and A. P. Makshtas, 2000: Low-level atmospheric jets and inversions over the Western Weddell Sea. *Bound.-Layer Meteor.,* **97,** 459–486.

Baas, P., S. R. de Roode, and G. Lenderink, 2008: The scaling behaviour of a turbulent kinetic energy closure model for stably stratified conditions. *Bound.-Layer Meteor.,* **127,** 17–36, doi:10.1007/s10546-007-9253-y.

Banta, R. M., and Coauthors, 1998: Daytime buildup and nighttime transport of urban ozone in the boundary layer during a stagnation episode. *J. Geophys. Res.,* **103,** 22 519–22 544.

——, R. K. Newsom, J. K. Lundquist, Y. L. Pichugina, R. L. Coulter, and L. Mahrt, 2002: Nocturnal low-level jet characteristics over Kansas during CASES-99. *Bound.-Layer Meteor.,* **105,** 221–252.

——, Y. L. Pichugina, and R. K. Newsom, 2003: Relationship between low-level jet properties and turbulence kinetic energy in the nocturnal stable boundary layer. *J. Atmos. Sci.,* **60,** 2549–2555.

——, ——, and W. A. Brewer, 2006: Turbulent velocity-variance profiles in the stable boundary layer generated by a nocturnal low-level jet. *J. Atmos. Sci.,* **63,** 2700–2719.

Beljaars, A. C. M., and F. C. Bosveld, 1997: Cabauw data for the validation of land surface parameterization schemes. *J. Climate,* **10,** 1172–1193.

Beyrich, F., 1994: Sodar observations of the stable boundary layer height in relation to the nocturnal low-level jet. *Meteor. Z.,* **3,** 29–34.

Blackadar, A. K., 1957: Boundary layer wind maxima and their significance for the growth of nocturnal inversions. *Bull. Amer. Meteor. Soc.,* **38,** 283–290.

Bonner, W. D., 1968: Climatology of the low level jet. *Mon. Wea. Rev.,* **96,** 833–850.

Bosveld, F. C., and F. Beyrich, 2004: Classifying observations of stable boundary layers for model validation. Preprints, *16th Symp. on Boundary Layers and Turbulence,* Portland, ME, Amer. Meteor. Soc., P4.13. [Available online at http://ams.confex.com/ams/pdfpapers/78641.pdf.]

Castro, C. L., R. A. Pielke Sr., and J. O. Adegoke, 2007: Investigation of the summer climate of the contiguous United States and Mexico using the Regional Atmospheric Modeling System (RAMS). Part I: Model climatology (1950–2002). *J. Climate,* **20,** 3844–3865.

Cheinet, S., A. Beljaars, M. Köhler, J. J. Morcrette, and P. Viterbo, 2005: Assessing physical processes in the ECMWF model forecasts using ARM SGP observations. ARM Rep. Series 1, ECMWF, 25 pp.

Chimonas, G., 2005: The nighttime accelerations of the wind in the boundary layer. *Bound.-Layer Meteor.,* **116,** 519–531.

Conangla, L., and J. Cuxart, 2006: On the turbulence in the upper part of the low-level jet: An experimental and numerical study. *Bound.-Layer Meteor.,* **118,** 379–400.

Cuxart, J., and Coauthors, 2006: Single-column model intercomparison for a stably stratified atmospheric boundary layer. *Bound.-Layer Meteor.,* **118,** 273–303.

Gaffard, C., L. Bianco, V. Klaus, and M. Matabuena, 2006: Evaluation of moments from wind profiler spectra: A comparison between five different processing techniques. *Meteor. Z.,* **15,** 73–85.

Garratt, J. R., 1985: Inland boundary layer at low latitudes. Part 1, the nocturnal jet. *Bound.-Layer Meteor.,* **32,** 307–327.

Ghan, S. J., X. Bian, and L. Corsetti, 1996: Simulation of the Great Plains low-level jet and associated clouds by general circulation models. *Mon. Wea. Rev.,* **124,** 1388–1408.

Holton, J. R., 1967: The diurnal boundary layer wind oscillation above sloping terrain. *Tellus,* **19,** 199–205.

Holtslag, A. A. M., 2006: GEWEX atmospheric boundary-layer study (GABLS) on stable boundary layers. *Bound.-Layer Meteor.,* **118,** 85–110.

——, and H. A. R. de Bruin, 1988: Applied modelling of the nighttime surface energy balance over land. *Bound.-Layer Meteor.,* **27,** 689–704.

Jiang, X., N. C. Lau, I. M. Held, and J. J. Ploshay, 2007: Mechanisms of the Great Plains low-level jet as simulated in an AGCM. *J. Atmos. Sci.,* **64,** 532–547.

Kaimal, J. C., and J. E. Gaynor, 1991: Another look at sonic thermometry. *Bound.-Layer Meteor.,* **56,** 401–410.

Karipot, A., M. Y. Leclerc, G. Zhang, T. Martin, G. Starr, D. Hollinger, J. H. McCaughey, and G. R. Hendrey, 2006: Nocturnal CO_2 exchange over a tall forest canopy associated with intermittent low-level jet activity. *Theor. Appl. Climatol.,* **85,** 243–248.

Klein Baltink, H., 1998: A long-term intercomparison of wind-profiler/RASS and tower measurements. *Meteor. Z.,* **7,** 271–279.

Kotroni, V., and K. Lagouvardos, 1993: Low-level jet streams associated with atmospheric cold fronts: Seven case studies selected from the FRONTS 87 experiment. *Geophys. Res. Lett.,* **20,** 1371–1374.

Kraus, H., J. Malcher, and E. Schaller, 1985: A nocturnal low-level jet during PUKK. *Bound.-Layer Meteor.,* **31,** 187–195.

Kurzeja, R. J., S. Berman, and A. H. Weber, 1991: A climatological study of the nocturnal planetary boundary layer. *Bound.-Layer Meteor.,* **54,** 105–128.

Lundquist, J. K., 2003: Intermittent and elliptical inertial oscillations in the atmospheric boundary layer. *J. Atmos. Sci.,* **60,** 2661–2673.

Maddox, R. A., 1983: Large-scale meteorological conditions associated with mid-latitude mesoscale convective complexes. *Mon. Wea. Rev.,* **111,** 1475–1493.

Mahrt, L., J. Sun, W. Blumen, W. Delany, and S. Oncley, 1998: Nocturnal boundary layer regimes. *Bound.-Layer Meteor.,* **88,** 255–278.

Mathieu, N., I. B. Strachan, M. Y. Leclerc, A. Karipot, and E. Pattey, 2005: Role of low-level jets and boundary layer properties on the NBL budget technique. *Agric. For. Meteor.,* **135,** 35–43.

McNider, R. T., and R. A. Pielke, 1981: Diurnal boundary layer development over sloping terrain. *J. Atmos. Sci.,* **38,** 2198–2212.

Monteith, J. L., 1981: Evaporation and surface temperature. *Quart. J. Roy. Meteor. Soc.,* **107,** 1–27.

Ohya, Y., R. Nakamura, and T. Uchida, 2008: Intermittent bursting of turbulence in a stable boundary layer with low-level jet. *Bound.-Layer Meteor.,* **126,** 349–363.

Parish, T. R., A. R. Rodi, and R. D. Clark, 1988: A case study of the summertime Great Plains low level jet. *Mon. Wea. Rev.,* **116,** 94–105.

Rama Krishna, T. V. B. P. S., M. Sharan, S. G. Gopalakrishnan, and Aditi, 2003: Mean structure of the nocturnal boundary layer under strong and weak wind conditions: EPRI case study. *J. Appl. Meteor.,* **42,** 952–969.

Smedman, A.-S., M. Tjernström, and U. Högström, 1993: Analysis of the turbulence structure of a marine low-level jet. *Bound.-Layer Meteor.,* **66,** 105–126.

Song, J., K. Liao, R. L. Coulter, and B. M. Lesht, 2005: Climatology of the low-level jet at the southern Great Plains Atmospheric Boundary Layer Experiment Site. *J. Appl. Meteor.,* **44,** 1593–1606.

Stensrud, D. J., 1996: Importance of low-level jets to climate: A review. *J. Climate,* **9,** 1698–1711.

Storm, B., J. Dudhia, S. Basu, A. Swift, and I. Giammanco, 2008: Evaluation of the Weather Research and Forecasting Model on forecasting low-level jets: Implications for wind energy. *Wind Energy,* **12,** 81–90, doi:10.1002/we.288.

Stull, R. B., 1988: *An Introduction to Boundary Layer Meteorology*. Kluwer Academic, 666 pp.

Svensson, G., and A. A. M. Holtslag, 2009: Analysis of model results for the turning of the wind and related momentum fluxes in the stable boundary layer. *Bound.-Layer Meteor.,* **132,** 261–277.

Thorpe, A. J., and T. H. Guymer, 1977: The nocturnal jet. *Quart. J. Roy. Meteor. Soc.,* **103,** 633–653.

Tijm, A. B. C., A. A. M. Holtslag, and A. J. van Delden, 1999: Observations and modeling of the sea breeze with the return current. *Mon. Wea. Rev.,* **127,** 625–640.

Todd, M. C., R. Washington, S. Raghavan, G. Lizcano, and P. Knippertz, 2008: Regional model simulations of the Bodélé low-level jet of northern Chad during the Bodélé Dust Experiment (BoDEx 2005). *J. Climate,* **21,** 995–1012.

Uppala, S. M., and Coauthors, 2005: The ERA-40 Re-Analysis. *Quart. J. Roy. Meteor. Soc.,* **131,** 2961–3012.

Van Delden, A. J., 1993: Observational evidence of the wave-like character of the sea breeze effect. *Beitr. Phys. Atmos.,* **66,** 63–72.

Van de Wiel, B. J. H., R. J. Ronda, A. F. Moene, H. A. R. de Bruin, and A. A. M. Holtslag, 2002: Intermittent turbulence and oscillations in the stable boundary layer over land. Part I: A bulk model. *J. Atmos. Sci.,* **59,** 942–958.

Van Ulden, A. P., and A. A. M. Holtslag, 1985: Estimation of atmospheric boundary layer parameters for diffusion applications. *J. Climate Appl. Meteor.,* **24,** 1196–1207.

——, and J. Wieringa, 1996: Atmospheric boundary layer research at Cabauw. *Bound.-Layer Meteor.,* **78,** 39–69.

Verkaik, J. W., and A. A. M. Holtslag, 2007: Wind profiles, momentum fluxes and roughness lengths at Cabauw revisited. *Bound.-Layer Meteor.,* **122,** 701–719.

Whiteman, C. D., X. Bian, and S. Zhong, 1997: Low-level jet climatology from enhanced rawinsonde observations at a site in the Southern Great Plains. *J. Appl. Meteor.,* **36,** 1363–1376.

Wilczak, J. M., M. L. Cancillo, and C. W. King, 1997: A wind profiler climatology of boundary layer structure above the boreal forest. *J. Geophys. Res.,* **102,** 29 083–29 100.

Wippermann, F., 1973: Numerical study on the effects controlling the low-level jet. *Beitr. Phys. Atmos.,* **46,** 137–154.

Zhang, K., and Coauthors, 2001: Numerical investigation of boundary layer evolution and nocturnal low-level jets: Local versus non-local PBL schemes. *Environ. Fluid Mech.,* **1,** 171–208.

Zhong, S., J. D. Fast, and X. Bian, 1996: A case study of the Great Plains low-level jet using wind profiler network data and a high-resolution mesoscale model. *Mon. Wea. Rev.,* **124,** 785–806.